



# Graphene–MoS<sub>2</sub> hybrid nanostructures enhanced surface plasmon resonance biosensors



Shuwen Zeng<sup>a,b</sup>, Siyi Hu<sup>b,d</sup>, Jing Xia<sup>c</sup>, Tommy Anderson<sup>b</sup>, Xuan-Quyen Dinh<sup>a</sup>, Xiang-Min Meng<sup>c</sup>, Philippe Coquet<sup>a,e</sup>, Ken-Tye Yong<sup>a,b,\*</sup>

<sup>a</sup> CINTRA CNRS/NTU/THALES, UMI 3288, Research Techno Plaza, 50 Nanyang Drive, Border X Block, Singapore 637553, Singapore

<sup>b</sup> School of Electrical and Electronic Engineering, Nanyang Technological University, Singapore 639798, Singapore

<sup>c</sup> Key Laboratory of Photochemical Conversion and Optoelectronic Materials, Technical Institute of Physics and Chemistry, Chinese Academy of Sciences, Beijing, China

<sup>d</sup> School of Science, Changchun University of Science and Technology, Changchun 130022, Jilin, China

<sup>e</sup> Institut d'Electronique, de Microélectronique et de Nanotechnologie (IEMN), CNRS UMR 8520 – Université de Lille 1, 59650 Villeneuve d'Ascq, France

## ARTICLE INFO

### Article history:

Received 14 August 2014

Received in revised form 22 October 2014

Accepted 28 October 2014

Available online 3 November 2014

### Keywords:

Surface plasmon resonance

Optical sensor

Graphene

MoS<sub>2</sub>

Differential phase

Enhanced biosensing

## ABSTRACT

In this work, we propose a new configuration of surface plasmon resonance (SPR) sensor that is based on graphene–MoS<sub>2</sub> hybrid structures for ultrasensitive detection of molecules. The proposed system displays a phase-sensitivity enhancement factor of more than 500-fold when compared to the SPR sensing scheme without the graphene–MoS<sub>2</sub> coating or with only graphene coating. Our hypothesis is that the monolayer MoS<sub>2</sub> has a much higher optical absorption efficiency (~5%) than that of the graphene layer (~2.3%). Based on our findings, the electron energy loss of MoS<sub>2</sub> layer is comparable to that of graphene and this will allow a successful (~100%) of light energy transfer to the graphene–MoS<sub>2</sub> coated sensing substrate. Such process will lead to a significant enhancement of SPR signals. Our simulation shows that a quasi-dark point of the reflected light can be achieved under this condition and this has resulted in a steep phase jump at the resonance angle of our newly proposed SPR system. More importantly, we found that phase interrogation detection approach of the graphene–MoS<sub>2</sub> hybrid structures-based sensing system is more sensitive than that of using the regularly angular interrogation method and our theoretical analysis indicates that 45 nm of Au film thickness and 3 coating layers of MoS<sub>2</sub> nanosheet are the optimized parameters needed for the proposed SPR system to achieve the highest detection sensitivity range.

© 2014 Elsevier B.V. All rights reserved.

## 1. Introduction

Two-dimensional (2D) nanomaterials have received great attention from the nanotechnology community in recent years due to their potential applications ranging from transistors to photodetectors [1–10]. For example, graphene is one of the most extensively studied 2D nanomaterial to date since its first discovery in 2004 [11]. It is considered as the thinnest man-made material (~0.34 nm) that is only composed of a single layer of hexagonally arranged carbon atoms and it is also known as the one of the strongest materials with a high breaking strength of 42 N/m which is at least 2 orders of magnitude stronger than that of the common steel. This unique intrinsic mechanical property makes graphene

a promising 2D nanomaterial for cost-effective fabrication of high-quality sensing substrates and display screens. Although graphene is known as the building block for a wide range of carbon materials such as 0D fullerene, 1D carbon nanotubes (CNTs) and 3D bulk graphite, its electronic and optical properties are significantly different when compared to allotropes mentioned above. For instance, the charge carrier mobility of graphene is reported to be as high as  $10^6 \text{ cm}^2 \text{ V}^{-1} \text{ s}^{-1}$  [12]. Thus, when graphene layers are deposited on metallic thin films or functionalized with metallic nanoparticles (e.g., Au or Ag), strong coupling can be induced at the metallic/graphene interface due to the effective charge transfer and this generates a large electric field enhancement at the nano-interface [13–18]. The electric field excited on the metallic surface is an evanescent wave and is sensitive toward the refractive-index change of its surrounding media. This phenomenon is generally referred as surface plasmon resonance (SPR). SPR sensors are the commonly used optical sensors for real-time monitoring of various biomolecular interactions such as DNA hybridization and protein bindings [2,19–21]. Recent studies have shown that graphene can

\* Corresponding author at: CINTRA CNRS/NTU/THALES, UMI 3288, Research Techno Plaza, 50 Nanyang Drive, Border X Block, Singapore 637553, Singapore.  
Tel.: +65 67905444.

E-mail addresses: [ktyong@ntu.edu.sg](mailto:ktyong@ntu.edu.sg), [imkentye@gmail.com](mailto:imkentye@gmail.com) (K.-T. Yong).

be used as an enhanced SPR substrate for biosensing applications. There are several advantages for using graphene-based SPR substrate for sensing: (i) they are able to induce significantly large field enhancement at the substrate interface; (ii) graphene has relatively large surface area ( $\sim 2630 \text{ m}^2 \text{ g}^{-1}$ ) thus allowing it to have a better surface contact with the analyte; and (iii) graphene surface can selectively detect aromatic compounds through pi-stacking force and this will help one to be able to study challenging experiments such as DNA interaction with proteins at extreme dilute condition [22–24]. However, it was reported that graphene-based SPR sensors possessed the highest detection sensitivity when the total number of graphene layers deposited on the metallic SPR sensing substrate (50 nm) is larger than 10. Even with such thick layers of graphene on the SPR substrate, the sensitivity enhancement factor has only increased from 1.25 to 2, which is considered to be an incremental improvement for the sensitivity of the SPR biosensor [22,25–28]. This incremental enhancement factor is mainly attributed to: (i) the angular-interrogation measurement method is generally used in these reported experiments where the change of resonance angle with the index perturbation on the sensing surface is proportional to the thickness of the high-refractive-index dielectric layer coated onto the Au thin film; and (ii) the low optical absorption ( $\sim 2.3\%$ ) of graphene [29,30] is not able to absorb sufficient energy to promote the excitation process of an efficient charge transfer between graphene and the metallic thin film. It is also worth noting that one can increase the thickness of metallic thin film to reduce the needed number of graphene layers (e.g., 60 nm silver thin film coated with monolayer graphene) [25] for sensing, but this will result in a much higher fabrication cost for preparing the SPR sensing substrate. Thus, this indicates that new alternative SPR sensing substrates must be developed to further push the envelope of the sensitivity of the SPR system.

More recently, ultra-thin layer of molybdenum disulfide ( $\text{MoS}_2$ ) that belongs to the transition-metal dichalcogenide (TMDC) semiconductor group is known as “beyond graphene” 2D nanocrystals material [31–33] and they are widely used as solid lubricants due to its low friction property. These 2D crystals composed of two-dimensional layers stacked in the vertical direction via van der Waals force. Similar to graphene, monolayer  $\text{MoS}_2$  can be prepared by micromechanical cleavage or synthesized using chemical vapor deposition (CVD) method [8,34]. When the thickness of  $\text{MoS}_2$  crystal is thinned down to monolayer ( $\sim 0.65 \text{ nm}$ ), a new set of electronic and optical property can be obtained. For example, bulk  $\text{MoS}_2$  has an indirect bandgap of 1.2 eV while monolayer  $\text{MoS}_2$  has a direct bandgap of 1.8 eV due to quantum confinement effects [35,36]. This unique feature allows  $\text{MoS}_2$  to serve as the nano-transistor channel with larger switching on/off ratios [8,33]. Also, monolayer of  $\text{MoS}_2$  possessed a high optical absorption efficiency ( $\sim 5\%$ ) that can be utilized to fabricate ultrasensitive photodetectors with a responsivity up to  $5 \times 10^8 \text{ A W}^{-1}$  [34,36–38]. Based on these unique features of  $\text{MoS}_2$  nanosheets, we proposed and designed a new configuration of enhanced SPR biosensors that is based on graphene– $\text{MoS}_2$  hybrid structures as shown in Fig. 1. The designed SPR sensing substrate consists of Au thin film and the film is coated with  $\text{MoS}_2$  nanosheets and monolayer graphene. Since the work function of Au (5.54 eV) is higher than that of  $\text{MoS}_2$  and graphene (5.1 eV and 4.5 eV), successful transfer of electrons from  $\text{MoS}_2$ /graphene hybrid layers to Au film will occur under optical excitation [39–41]. This process will lead to a larger electric field enhancement at the sensing interface thereby resulting in a higher sensitivity to the target analytes [2]. In our proposed system,  $\text{MoS}_2$  layers are used for improving the light absorption in order to provide enough excitation energy for effective charge transfer, while monolayer graphene is acting as bio-recognition component for capturing the target biomolecules through pi-stacking force. In this study, the SPR sensing performance is systematically investigated by varying the thickness of Au

thin film and number of  $\text{MoS}_2$  layers using transfer-matrix analysis. Since the Heaviside step-like phase changes are much sharper than the resonance angle shift, the sensitivity enhancement of our proposed system can be significantly improved. In our theoretical analysis, we show that the sharpest phase signal change and lowest value of minimum reflectivity can be achieved when SPR substrate of 45 nm Au thin film coated by 3 layers of  $\text{MoS}_2$  and 1 monolayer of graphene is used. The phase sensitivity of this system is increased by more than 2 orders when compared to those sensing substrate with “naked” Au thin film or Au thin film coated with graphene.

## 2. Design consideration and theoretical model

In our proposed new configuration, a well-known Kretschmann configuration is employed [20], where the Au thin film coated glass slide is attached to the base of an equilateral prism made of high refractive index glass through index matching fluid. Before the attachment to prism, graphene and  $\text{MoS}_2$  layers are deposited on the top of the Au thin film coated glass slide [9,42,43]. The excitation light wavelength used for the SPR sensing is 632.8 nm. The TM-polarized light is incident from one lateral face of the prism, then reached to its base and totally reflected out from the other lateral face and collected and analyzed by a photodetector.

### 2.1. Refractive index of various layer components

The first layer is the SF11 prism and its refractive index ( $n_1$ ) is calculated through the following relation [44]:

$$n_1 = \left( \frac{1.73759695\lambda^2}{\lambda^2 - 0.013188707} + \frac{0.313747346\lambda^2}{\lambda^2 - 0.0623068142} + \frac{1.89878101\lambda^2}{\lambda^2 - 155.23629} + 1 \right)^{1/2} \quad (1)$$

where  $\lambda$  is the wavelength of incident light in  $\mu\text{m}$ . Eq. (1) is valid for wavelengths ranging from 0.37 to 2.50  $\mu\text{m}$ . Similarly, the second layer is the BK7 glass slide and its refractive index ( $n_2$ ) is determined by the following relation [44]:

$$n_2 = \left( \frac{1.03961212\lambda^2}{\lambda^2 - 0.00600069867} + \frac{0.231792344\lambda^2}{\lambda^2 - 0.0200179144} + \frac{1.01046945\lambda^2}{\lambda^2 - 103.560653} + 1 \right)^{1/2} \quad (2)$$

where  $\lambda$  is the wavelength of incident light in  $\mu\text{m}$ . Eq. (2) is valid for wavelengths ranging from 0.30 to 2.50  $\mu\text{m}$ . The complex refractive index of titanium adhesion layer ( $n_3$ ) at 632.8 nm is obtained from the experimental measurement data by Palik [45]. The fourth layer is the Au thin film and its complex refractive index ( $n_4$ ) is calculated through the Drude model as follows [46,47]:

$$n_4 = (\varepsilon_{4r} + i\varepsilon_{4i})^{1/2} = \left( 1 - \frac{\lambda^2 \lambda_c}{\lambda_p^2(\lambda_c + i\lambda)} \right)^{1/2} \quad (3)$$

where  $\lambda_p$  ( $1.6826 \times 10^{-7} \text{ m}$ ) and  $\lambda_c$  ( $8.9342 \times 10^{-6} \text{ m}$ ) represent the plasma and the collision wavelengths of gold, respectively. The complex refractive index of monolayer  $\text{MoS}_2$  ( $n_5$ ) at 632.8 nm is obtained from the experimental measurement data by Castellanos-Gomez et al. [48] and the thickness of  $\text{MoS}_2$  layers ( $d_5 = L \times 0.65 \text{ nm}$ ) [35], where  $L$  is the number of  $\text{MoS}_2$  layer. The sixth layer of our model is monolayer graphene ( $d_6 = 0.34 \text{ nm}$ ) and its complex refractive index ( $n_6$ ) in the visible range is given as [49]:

$$n_6 = 3.0 + i \frac{C_1}{3} \lambda \quad (4)$$

where the constant  $C_1 \approx 5.446 \mu\text{m}^{-1}$  [29] and  $\lambda$  is the wavelength of incident light in  $\mu\text{m}$ . The sensing medium for initial calibration is deionized (DI) water and its refractive index ( $n_7$ ) is determined by the following relation [50]:

$$n_7^2 - 1 = \sum_{i=1}^4 \frac{A_i \lambda^2}{\lambda^2 - t_i^2} \quad (5)$$

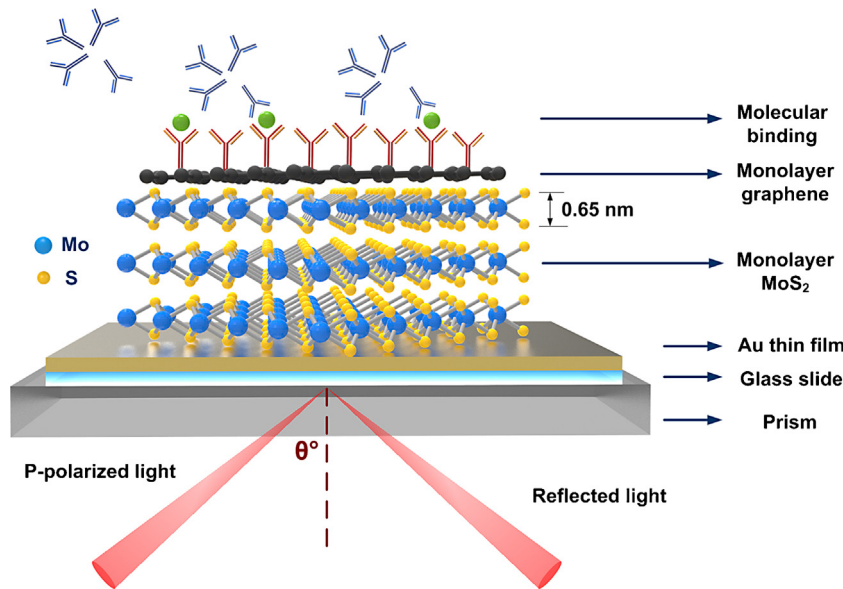


**Fig. 1.** Schematic diagram of graphene–MoS<sub>2</sub> enhanced SPR biosensor.

where the Sellmeier coefficients  $A_1 = 5.666959820 \times 10^{-1}$ ,  $A_2 = 1.731900098 \times 10^{-1}$ ,  $A_3 = 2.095951857 \times 10^{-2}$ ,  $A_4 = 1.125228406 \times 10^{-1}$ ,  $t_1 = 5.084151894 \times 10^{-3}$ ,  $t_2 = 1.818488474 \times 10^{-2}$ ,  $t_3 = 2.625439472 \times 10^{-2}$ ,  $t_4 = 1.073842352 \times 10^1$  and  $\lambda$  is the wavelength of incident light in  $\mu\text{m}$ . Eq. (5) is valid for wavelengths ranging from 0.182 to 1.129  $\mu\text{m}$ . The refractive-index change of the sensing medium induced by the adsorption of biomolecules on the surface of monolayer graphene is denoted by  $\Delta n_{bio}$ . Thus, based on the above parameters and equations, the refractive indices of the seven layers used in our SPR modeling at 632.8 nm are respectively:  $n_1 = 1.7786$ ,  $n_2 = 1.5151$ ,  $n_3 = 2.1526 + i2.9241$ ,  $n_4 = 0.1838 + i3.4313$ ,  $n_5 = 5.9000 + i0.8000$ ,  $n_6 = 3.0000 + i1.1487$ ,  $n_7 = 1.3320 + \Delta n_{bio}$ .

## 2.2. Phase ( $\phi_p$ ) and reflectivity ( $R_p$ )

To systematically investigate the phase and reflectivity change in our graphene–MoS<sub>2</sub> hybrid structure based SPR sensing system, we employed the transfer matrix method (TMM) and Fresnel equations based on an  $N$ -layer model to perform a detailed analysis. The layers are parallelly stacked along in the  $Z$ -direction that is perpendicular to the sensing interface and each layer is defined by their respective dielectric constant ( $\varepsilon = n^2$ ) and thickness ( $d$ ). All layers are set to be optically isotropic and non-magnetic. The electromagnetic fields at the first boundary  $Z_1$  in the tangential direction is set as  $Z = Z_1 = 0$ . And the relation of the tangential fields of the last boundary  $Z_{N-1}$  and the first boundary  $Z_1$  is given as [22,46]:

$$\left[ \begin{array}{c} U_1 \\ V_1 \end{array} \right] = M \left[ \begin{array}{c} U_{N-1} \\ V_{N-1} \end{array} \right] \quad (6)$$

where  $U_1$  and  $U_{N-1}$  are respectively the tangential component of electric field at the boundary of the first layer and the  $N$ th layer,  $V_1$  and  $V_{N-1}$  are respectively the tangential component of magnetic field at the boundary of the first layer and the  $N$ th layer,  $M$  is known as the characteristic Transfer Matrix (TM) of the combined  $N$ -layer structure and can be obtained through the following relation for the  $p$ -polarization light [51,52]:

$$M = \prod_{k=2}^{N-1} M_k = \begin{bmatrix} M_{11} & M_{12} \\ M_{21} & M_{22} \end{bmatrix} \quad (7)$$

with

$$M_k = \begin{bmatrix} \cos \beta_k & (-i \sin \beta_k)/q_k \\ -iq_k \sin \beta_k & \cos \beta_k \end{bmatrix} \quad (8)$$

where

$$q_k = \left( \frac{\mu_k}{\varepsilon_k} \right)^{1/2} \cos \theta_k = \frac{(\varepsilon_k - n_1^2 \sin^2 \theta_1)^{1/2}}{\varepsilon_k} \quad (9)$$

and

$$\beta_k = \frac{2\pi}{\lambda} n_k \cos \theta_k (z_k - z_{k-1}) = \frac{2\pi d_k}{\lambda} (\varepsilon_k - n_1^2 \sin^2 \theta_1)^{1/2} \quad (10)$$

Here,  $\varepsilon_k$  and  $d_k$  represent the dielectric constant and thickness of the  $k$ th layer,  $\theta_1$  and  $\lambda$  are respectively the incident angle and wavelength at the base of SF11 prism as shown in Fig. 1. The total reflection coefficient ( $r_p$ ) for the  $p$ -polarization light is related to the matrix as follows:

$$r_p = \frac{(M_{11} + M_{12} q_N) q_1 - (M_{21} + M_{22} q_N)}{(M_{11} + M_{12} q_N) q_1 + (M_{21} + M_{22} q_N)} \quad (11)$$

where  $q_1$  and  $q_N$  are the corresponding terms for the first layer (SF11 prism) and  $N$ th layer (the sensing medium that contains the target biomolecules) from Eq. (9). Finally, the phase ( $\phi_p$ ) and reflectivity ( $R_p$ ) of the  $p$ -polarization light are obtained as:

$$\phi_p = \arg(r_p) \quad (12)$$

and

$$R_p = |r_p|^2 \quad (13)$$

For  $s$ -polarization light the above equations hold except:

$$q_k = \left( \frac{\varepsilon_k}{\mu_k} \right)^{1/2} \cos \theta_k = (\varepsilon_k - n_1^2 \sin^2 \theta_1)^{1/2} \quad (14)$$

It is known that SPR only affects  $p$ -polarization light (i.e., transverse magnetic waves), therefore  $s$ -polarization light (i.e., transverse electric waves) can be served as a reference signal to eliminate environmental noises for improving the stability and accuracy of SPR sensors throughout the measurement [20,47]. The differential phase between  $p$ - and  $s$ -polarization is obtained as  $\phi_d = |\phi_p - \phi_s|$ .

The plot of reflectivity ( $R_p$ ) versus incident angle ( $\theta_{inc}$ ) is called SPR curve, where the resonant dip angle ( $\theta_{SPR}$ ) corresponds to the

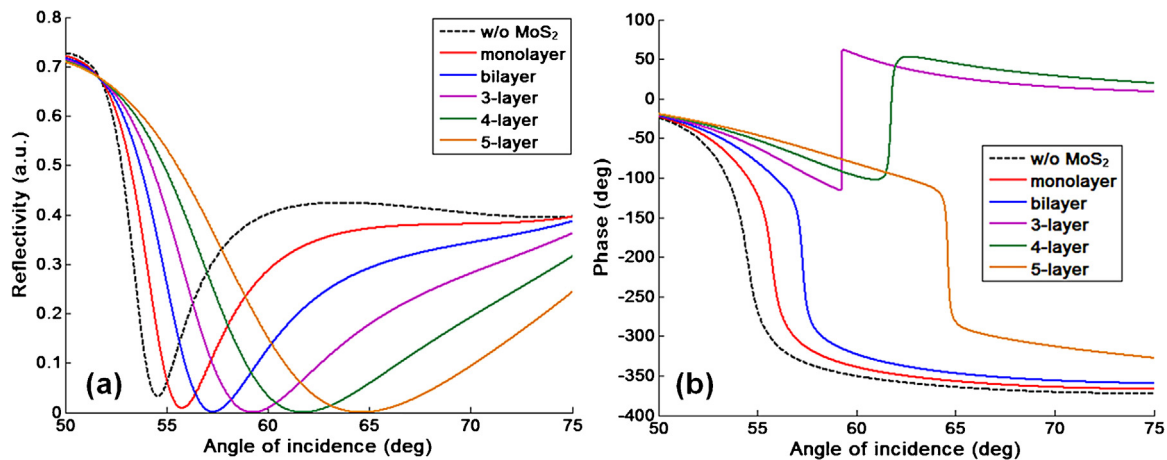


**Fig. 2.** Variation of (a) reflectivity and (b) phase with respect to angle of incidence for different number of MoS<sub>2</sub> layers with sensing layer refractive index 1.332 at wavelength 632.8 nm. The thickness of the gold layer is 45 nm.

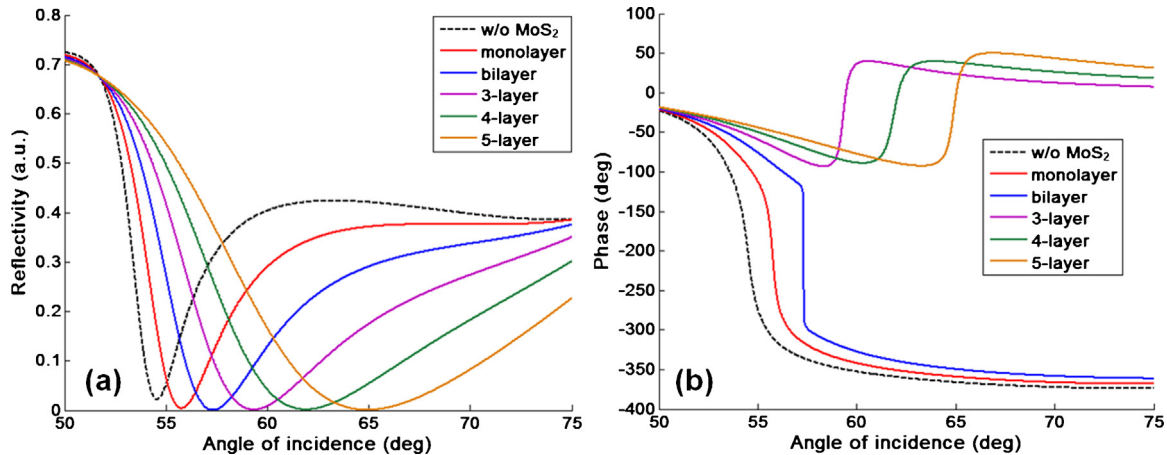


**Fig. 3.** Variation of (a) reflectivity and (b) phase with respect to angle of incidence for different number of MoS<sub>2</sub> layers with sensing layer refractive index 1.332 at wavelength 632.8 nm. The thickness of the gold layer is 46 nm. (For interpretation of the references to color in the text, the reader is referred to the web version of this article.)

minimum value of the reflectivity and changes with the refractive-index change  $\Delta n_{bio}$  of the sensing medium that is induced by the binding of the target biomolecules. The shift of the resonance angle is due to the wave vector matching (i.e., the SPR excitation condition) between the incident light along the direction of SP propagation ( $k_x$ ) and the surface plasmon waves ( $k_{SP}$ ) as follows:

$$k_x = k_{SP} \quad \text{with} \quad k_x = k_0 n_{prism} \sin \theta_{SPR} \quad \text{and}$$

$$k_{SP} = Re \left[ k_0 \left( \frac{\varepsilon_{mmg} n_s^2}{\varepsilon_{mmg} + n_s^2} \right)^{1/2} \right] \quad (15)$$

where  $k_0$  is the wave vector of the incident light in free space,  $\varepsilon_{mmg}$  is the dielectric constant of the graphene-MoS<sub>2</sub> enhanced metallic thin film and  $n_s$  is the refractive index of the sensing medium that contains target biomolecules. It is worth noting that an abrupt

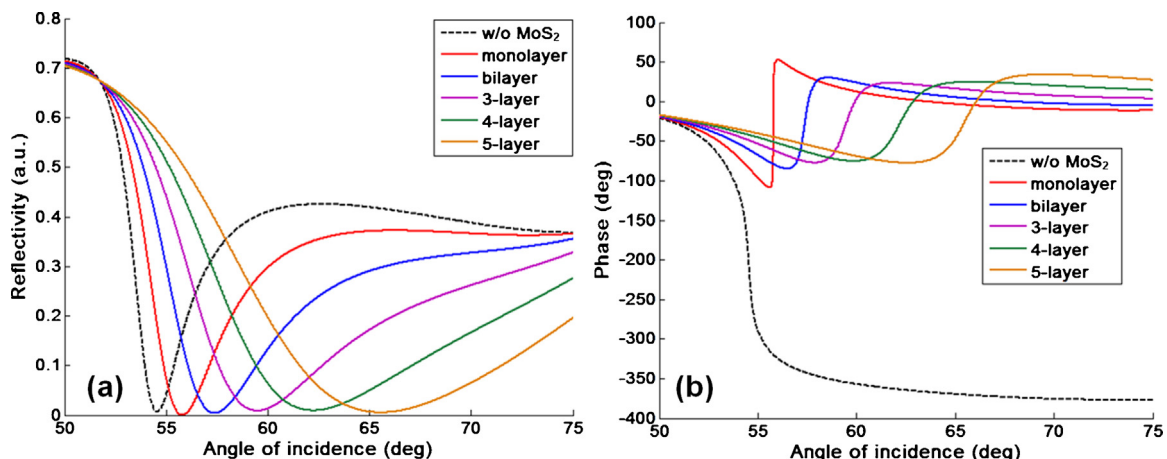


**Fig. 4.** Variation of (a) reflectivity and (b) phase with respect to angle of incidence for different number of MoS<sub>2</sub> layers with sensing layer refractive index 1.332 at wavelength 632.8 nm. The thickness of the gold layer is 48 nm. (For interpretation of the references to color in the text, the reader is referred to the web version of this article.)

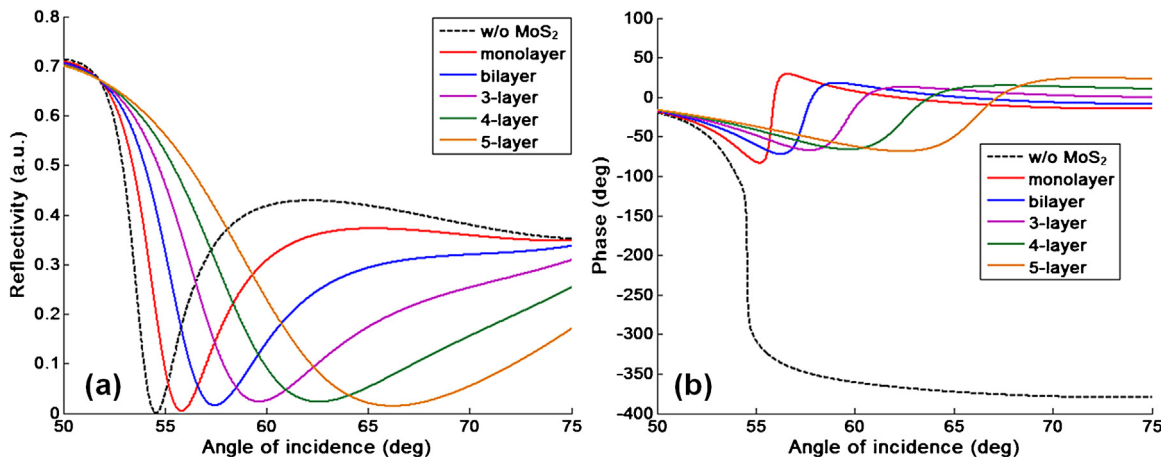


**Fig. 5.** Variation of (a) reflectivity and (b) phase with respect to angle of incidence for different number of MoS<sub>2</sub> layers with sensing layer refractive index 1.332 at wavelength 632.8 nm. The thickness of the gold layer is 50 nm.

phase change would occur at the resonant dip angle ( $\theta_{SPR}$ ) where the reflected light intensity is approaching zero (i.e., a point of quasi-darkness). The darker the reflectivity, the sharper the phase jump [53]. Thus, even a tiny refractive-index change that is induced by the flow in of target biomolecules solutions (1 nM to 1 pM) can be detected by the sharp phase signal ( $\Delta\phi_d$ ) measured at a fixed  $\theta_{SPR}$  corresponding to the initial calibration sensing medium. The SPR phase sensitivity ( $S_p$ ) is defined by:

$$S_p = \frac{\Delta\phi_d}{\Delta n_{bio}} \quad (16)$$

The enhancement factor ( $E_p$ ) of phase sensitivity with graphene–MoS<sub>2</sub> enhanced metallic thin film ( $S_{pmmg}$ ) against that of the pure metallic thin film ( $S_{pm}$ ) is given as:

$$E_p = \frac{S_{pmmg}}{S_{pm}} = \frac{\Delta\phi_{dmmg}/\Delta n_{bio}}{\Delta\phi_{dm}/\Delta n_{bio}} = \frac{\Delta\phi_{dmmg}}{\Delta\phi_{dm}} \quad (17)$$

where  $\Delta\phi_{dmmg}$  and  $\Delta\phi_{dm}$  are respectively the differential phase changes corresponding to  $\Delta n_{bio}$  with the graphene–MoS<sub>2</sub> enhanced metallic thin film and the pure metallic thin film.

### 3. Results and discussion

From Eqs. (16) and (17), one can see that the SPR phase sensitivity ( $S_p$ ) and enhancement factor ( $E_p$ ) of graphene–MoS<sub>2</sub> coated metallic thin film sensing substrate are essentially determined by the differential phase change ( $\Delta\phi_d$ ) for a fixed refractive index variation ( $\Delta n_{bio}$ ) induced by the molecular interaction on the sensing surface. The sharpest phase change of *p*-polarization light under SPR excitation condition only occurs at the point where the intensity of the reflected light is at the minimum that is close to zero [53,54]. Since there is a trade-off between the enhancement effect and the electron energy loss by inserting MoS<sub>2</sub> layers between monolayer graphene and Au thin film for achieving the minimum reflectivity, we first systematically investigated the effects of Au thickness and number of MoS<sub>2</sub> layer on the spectral reflectivity and phase of SPR curves and this can be achieved by using Eqs. (12) and (13). The refractive index of sensing medium is fixed at 1.332 that is corresponded to DI water.

There are three important features that can be observed from the graphene–MoS<sub>2</sub> SPR reflectivity curves (Figs. 2a–5a, Fig. S1a–S12a and Supplementary Video 1): (i) The SPR resonance angle ( $\theta_{SPR}$ ) has a large red shift with increasing number of MoS<sub>2</sub> layers at a fixed Au thin film thickness that is due to the large value of the real part of the MoS<sub>2</sub> dielectric function. According to the excitation condition in Eq. (15), increasing the real part of the MoS<sub>2</sub> dielectric function

will lead to an increase of the SP wavevector ( $k_{SP}$ ) (i.e., a decrease of the SP propagation velocity) [55]. As a result, a larger incident angle is required for the excitation of SPR; (ii) a rapid broadening of the curves is observed when the number of MoS<sub>2</sub> layers deposited on the Au thin film increases and this is caused by the electron energy loss of MoS<sub>2</sub> layers which is related to the imaginary part of their dielectric function (Fig. 7c). The imaginary part of dielectric function of MoS<sub>2</sub> layers is larger than that of Au thin film thus leading to a larger electron energy loss; (iii) the resonance depth (i.e., the value of minimum reflectivity) is strongly dependent on the number of MoS<sub>2</sub> layers coated on the Au thin film (Fig. 7d). More specifically, the light energy absorbed by Au thin film is insufficient to promote a strong SPR excitation. The resonance depth of Au film with thickness less than 45 nm is much higher than that of the Au film with thickness greater than 45 nm. By further coating MoS<sub>2</sub> layers on the surface of Au film, the light absorption of the Au–MoS<sub>2</sub> structure can be effectively enhanced and thereby promoting a stronger SPR excitation (Fig. S1a). However, the enhancement effect of MoS<sub>2</sub> layers is overwhelmed by the electron energy loss when additional layers were coated on Au thin film with a thickness of 50 nm and above. The lowest value of minimum reflectivity ( $1.2680 \times 10^{-8}$ ) is obtained when the Au thickness is set at 45 nm and 3-layers of MoS<sub>2</sub> are used. As shown in Figs. 2b–5b, Figs. S1b–S12b and Supplementary Video 2, the Heaviside step-like phase jumps occur at the resonance angle where the resonance depth is the lowest at a fixed Au thin film thickness. For example, the sharpest phase changes for Au thin film with thicknesses of 46 nm and 48 nm are at the point of their respective lowest values of minimum reflectivity which are induced by the bilayer (blue curve in Fig. 3) and monolayer of MoS<sub>2</sub> (red curve in Fig. 4). Thus, 45 nm Au thin film and 3 layers of MoS<sub>2</sub> layers are the optimal parameters that need to be used to achieve the best sensitivity of the proposed SPR sensing system. Also, we have calculated that the sharpest phase signal change takes place with a resonance angle of 59.2592° (see Fig. 6).

To compare the phase and angular sensing performance of the graphene–MoS<sub>2</sub> structure based SPR biosensor, we plotted out the differential phase change ( $\Delta\phi_d$ ) and resonance angle change ( $\Delta\theta_{SPR}$ ) at a fixed refractive-index change ( $\Delta n_{bio} = 0.0012$  or  $\Delta n_{bio} = 0.12$ ) that is induced by the target molecular binding at the sensing surface as illustrated in Fig. 7a and b. The results showed that the resonance angle change ( $\Delta\theta_{SPR}$ ) with a fixed  $\Delta n_{bio}$  is independent of the minimum reflectivity of the SPR curves before the adsorption of biomolecules and it increases with the increasing number of MoS<sub>2</sub> layers from 0 to 4 and subsequently saturated at 5 layers due to the loss by over-absorption of MoS<sub>2</sub> against its enhancement effect. The largest resonance angle change ( $\Delta\theta_{SPR}$ )

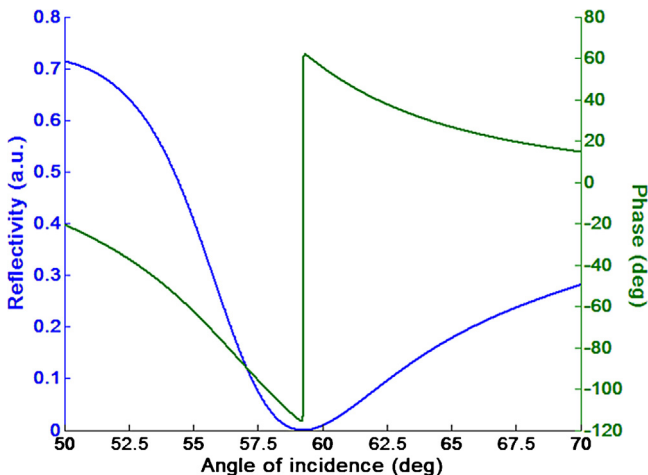


**Fig. 6.** Comparison of the reflectivity (blue) and phase (green) change as functions of the angle of light incidence with sensing layer refractive index 1.332 at wavelength 632.8 nm. The thickness of the gold layer is 45 nm and the number of MoS<sub>2</sub> layers is 3. Phase experiences a sharp singularity in the minimum of SPR curve. (For interpretation of the references to color in this figure legend, the reader is referred to the web version of this article.)

is  $\sim 3.3^\circ$  for a large refractive-index change of 0.12 and with 4-layers MoS<sub>2</sub> coated between the monolayer graphene and 55 nm Au thin film (green curve in Fig. 7b). In comparison to the angular signal variation, the differential phase changes ( $\Delta\phi_d$ ) are much

more significant for even a tiny refractive-index change of 0.0012. The optimized phase results are respectively  $51.0989^\circ$  for monolayer MoS<sub>2</sub> coated 48 nm Au thin film,  $67.6725^\circ$  for bilayer MoS<sub>2</sub> coated 46 nm Au thin film and  $98.2226^\circ$  for 3-layer MoS<sub>2</sub> coated 45 nm Au thin film. It is worth noting that the differential phase changes with graphene–MoS<sub>2</sub> coated Au thin films are all larger than that of the monolayer graphene coated Au thin film with an optimum thickness of 50 nm ( $\Delta\phi_d = 27.8046^\circ$ ), which demonstrates that the graphene–MoS<sub>2</sub> hybrid structure has a much better enhancement effect than that of the graphene material alone. If only graphene layers are deposited on the metallic thin film, the SPR signal enhancement effect will be compromised by the increment of electron energy loss in the system (see Figs. S13 and S14). We have summarized the sensing configurations and performances for the largest five differential phase changes to  $\Delta n_{bio} = 0.0012$  for all the combinations of the Au thickness ranging from 40 nm to 55 nm and the number of MoS<sub>2</sub> layers (0 to 5) in Table 1. The table also shows that the lower the value of the minimum reflectivity, the larger the differential phase change.

The phase signal changes to  $\Delta n_{bio}$  with different number of MoS<sub>2</sub> layers coated on Au thin film with thicknesses of 40 nm, 45 nm, 46 nm, 48 nm, 50 nm and 55 nm are shown in Fig. 8. The sensing signal for the configuration of 45 nm Au thin film coated with 3-layers MoS<sub>2</sub> and monolayer graphene exhibited a steep phase change from  $\Delta n_{bio} = 1.332$  to  $\Delta n_{bio} = 1.3322$  (purple curve in Fig. 8b), which shows great promise for detecting biomolecules with molecular weight less than 8 kDa or at concentration as low as 1 pM [22]. The incident angle for this sharp phase signal change is

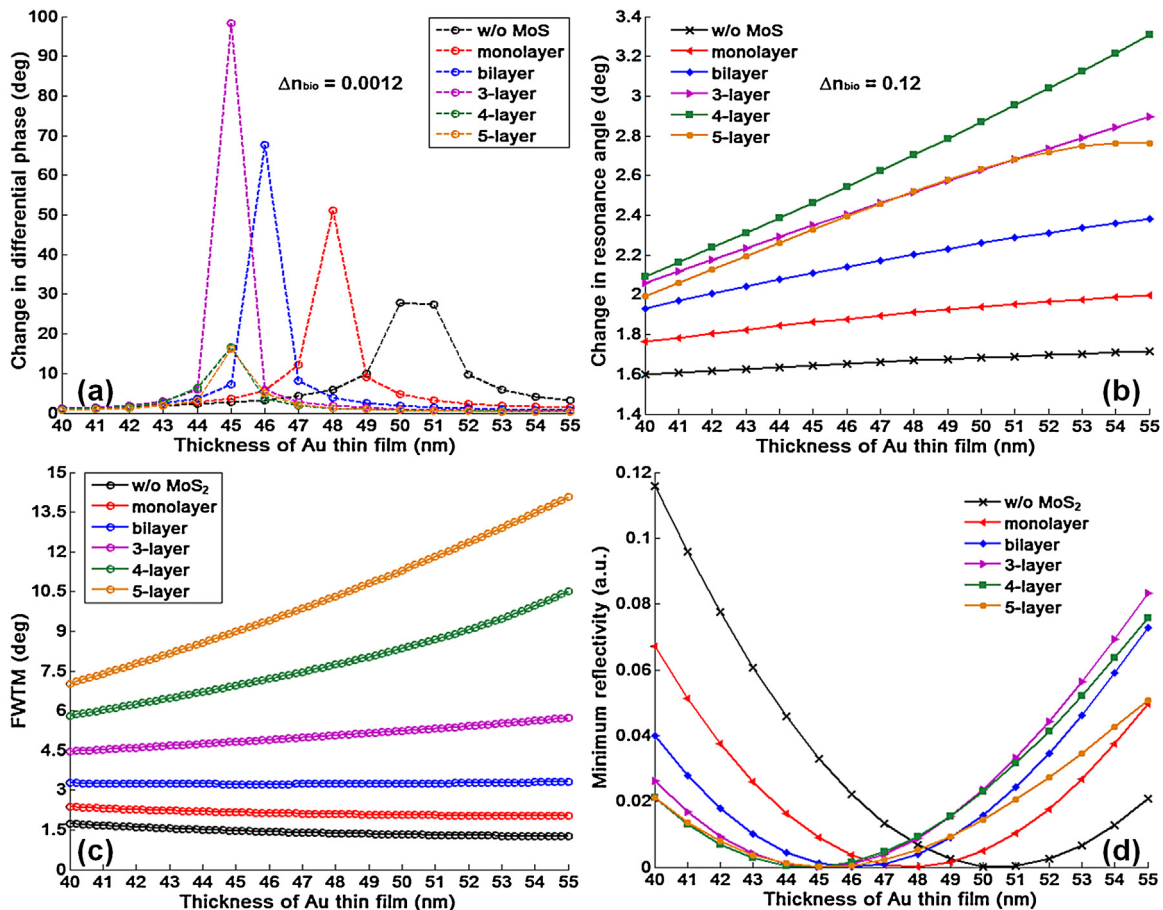


**Fig. 7.** Variation of change in (a) differential phase, (b) resonance angle due to the adsorption of biomolecules to the sensing surface, (c) FWTM and (d) minimum reflectivity in SPR curve with sensing layer refractive index 1.332, for various thicknesses of gold and different layers of MoS<sub>2</sub> at wavelength 632.8 nm. The symbols correspond to the values obtained from the simulated results while the continuous lines are the best-fit curves through these symbols. (For interpretation of the references to color in the text, the reader is referred to the web version of this article.)

**Table 1**

Optimized values of thickness of gold and the number of MoS<sub>2</sub> layers with corresponding change in resonance angle  $\Delta\theta_{SPR}$  and differential phase  $\Delta\phi_d$ .

Au thickness	Number of MoS <sub>2</sub> layers	$\theta_{SPR}$ w/o biomolecules	$\theta_{SPR}$ with biomolecules	$\Delta\theta_{SPR}$ ( $\Delta n_{bio} = 0.12$ )	$\Delta\phi_d$ ( $\Delta n_{bio} = 0.0012$ )	FWTM	Minimum reflectivity
45 nm	5	64.6186°	66.9486°	2.3300°	16.3305°	8.9808°	$3.1928 \times 10^{-5}$
45 nm	4	61.7380°	64.2028°	2.4648°	16.7458°	6.9507°	$7.6821 \times 10^{-5}$
45 nm	3	59.2592°	61.6090°	2.3498°	98.2226°	4.8269°	$1.2680 \times 10^{-8}$
46 nm	2	57.3250°	59.4671°	2.1421°	67.6725°	3.2275°	$1.9026 \times 10^{-6}$
48 nm	1	55.7940°	57.7043°	1.9103°	51.0989°	2.0956°	$2.7116 \times 10^{-5}$
50 nm	0	54.5661°	56.2499°	1.6838°	27.8046°	1.3260°	$2.6143 \times 10^{-4}$

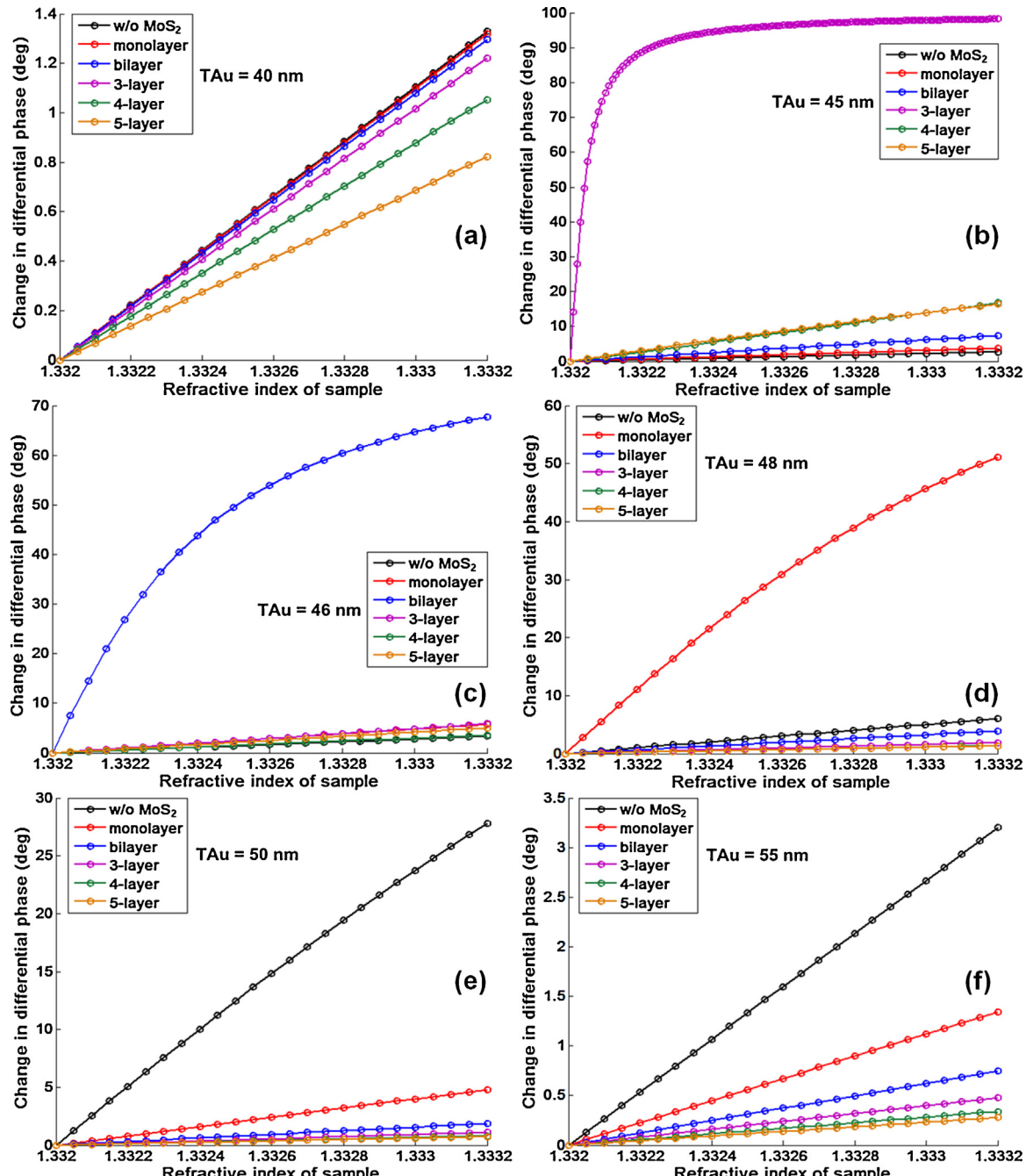


**Fig. 8.** Variation of change in differential phase with respect to sensing layer refractive index for different number of MoS<sub>2</sub> layers and a fixed thickness of gold layer: (a) 40 nm, (b) 45 nm, (c) 46 nm, (d) 48 nm, (e) 50 nm and (f) 55 nm at wavelength 632.8 nm. The symbols correspond to the values obtained from the simulated results while the continuous lines are the best-fit curves through these symbols. (For interpretation of the references to color in the text, the reader is referred to the web version of this article.)

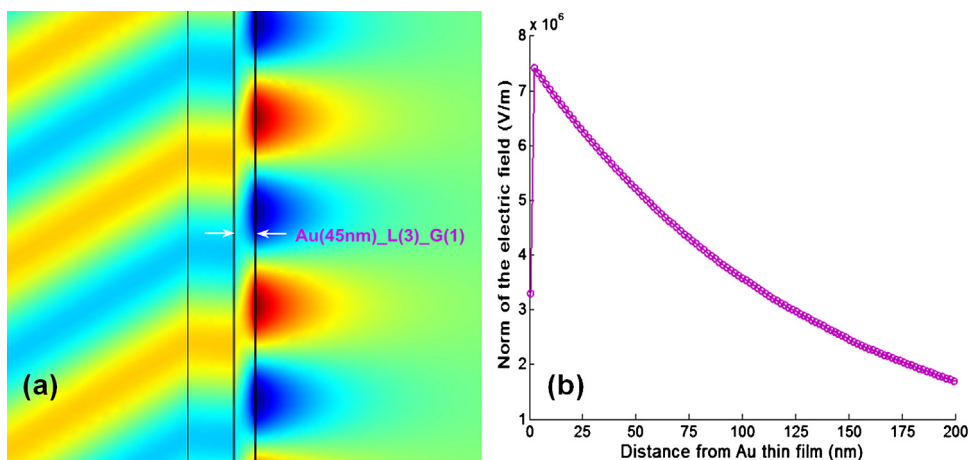


**Fig. 9.** FEA simulations of resonant graphene–MoS<sub>2</sub> enhanced Au sensing film. (a) Electric field distribution at the SPR resonance angle 59.2592°. (b) Cross-section plot of the total electric field along the direction perpendicular to the prism base, showing clear evanescent field at the sensing interface.

fixed at the SPR resonance angle of 59.2592°. If one wants to use this ultrasensitive configuration to detect a larger  $\Delta n_{bio}$ , one only needs to shift the incident angle  $\pm 0.001^\circ$  away from the resonance angle for a linear phase signal change or to choose other combinations of Au thin film thickness and number of MoS<sub>2</sub> layers like bilayer MoS<sub>2</sub>-coated 46 nm Au thin film (blue curve in Fig. 8c) or monolayer MoS<sub>2</sub>-coated 48 nm Au thin film (red curve in Fig. 8d) for achieving the best detection sensitivity. To further confirm the strong SPR excitation of 3-layers MoS<sub>2</sub> coated between monolayer graphene and 45 nm Au thin film, we employed finite element analysis (FEA) method (COMSOL Multiphysics 4.3a) to study the electric field distribution inside the graphene–MoS<sub>2</sub> structure based sensing system at the resonance angle (see Fig. 9). It can be seen that a large electric field enhancement is generated at the sensing surface and the probing field intensity exponentially decayed to the sensing medium that contains the target biomolecules with a penetration depth around 150 nm. The penetration depth is defined as the distance where the electric field is reduced to  $1/e$  of its value. Thus, the electric probing field close to the graphene

capture layer is very intense and highly sensitive to small biomolecule interactions. According to Eqs. (16) and (17), the SPR phase sensitivity is proportional to the differential phase change ( $\Delta\phi_d$ ) for a fixed  $\Delta n_{bio}$  and therefore the enhancement factor for the graphene–MoS<sub>2</sub> enhanced SPR biosensor is determined by the ratio of their differential phase change ( $\Delta\phi_{dmg}/\Delta\phi_{dm}$ ) for the same refractive index change that is induced by the target molecule bindings. The linear phase signal changes detected by the conventional SPR sensor with pure Au thin film, graphene-based SPR biosensor and graphene–MoS<sub>2</sub> based SPR biosensor for a tiny refractive-index change ( $\Delta n_{bio}$ ) as low as 10<sup>-6</sup> RIU are plotted in Fig. 10. The enhancement factor ( $E_p$ ) for the graphene–MoS<sub>2</sub> based SPR biosensor is calculated to have more than 500-fold of increment when compared to both the conventional and graphene based SPR sensors with the same thickness of Au thin film.

#### 4. Conclusions

In this study, a highly sensitive graphene–MoS<sub>2</sub> nanobiosensor based on differential phase measurement is presented. The sensing substrate consists of MoS<sub>2</sub> and graphene deposited Au thin film. Monolayer graphene acts as a bio-recognition component to selectively detect targeting biomolecules through pi-stacking force. In addition, our theoretical analysis shows that electron transfer due to the work functions difference between graphene, MoS<sub>2</sub> and Au will result in a large electric field enhancement at the sensing interface and thus leading to an ultrahigh sensitivity of the sensing system. Since monolayer MoS<sub>2</sub> had a higher light absorption rate than that of graphene, a stronger SPR excitation can be achieved by using the graphene–MoS<sub>2</sub> hybrid structure as the sensing substrate. In comparison to angular measurement that requires a large number of MoS<sub>2</sub> (5 to 10) to improve the sensitivity of the SPR system, phase detection only depends on the minimum reflectivity of the sensing system which allows one to use a fewer number of MoS<sub>2</sub> layers and an enhancement factor of more than 2 orders is demonstrated by using 3-layers MoS<sub>2</sub> and a monolayer graphene coated on the 45 nm Au thin film. Also, we have found that the width of the SPR reflectivity curves can be significantly reduced by using a fewer number of MoS<sub>2</sub> layers together with the phase interrogation detection method and this will provide higher detection accuracy for the system.

#### Appendix A. Supplementary data

Supplementary data associated with this article can be found, in the online version, at <http://dx.doi.org/10.1016/j.snb.2014.10.124>.

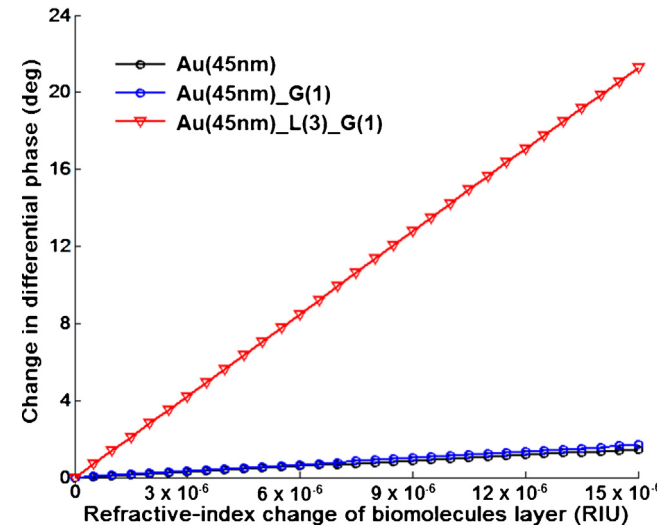


**Fig. 10.** Comparison of the SPR sensing performances with pure Au thin film, monolayer graphene coated Au thin film and monolayer graphene–MoS<sub>2</sub> coated Au thin film (3 layers of MoS<sub>2</sub>) for a tiny refractive-index change (as low as 10<sup>-6</sup> RIU) due to adsorption of biomolecules on the sensing surface. The differential phase signals for pure Au thin film and monolayer graphene coated Au thin film (black and blue curves) are magnified by a factor of 50 for clarity. (For interpretation of the references to color in this figure legend, the reader is referred to the web version of this article.)

## References

- [1] A.K. Geim, I.V. Grigorieva, Van der Waals heterostructures, *Nature* 499 (2013) 419–425.
- [2] S. Zeng, D. Baillargeat, H.-P. Ho, K.-T. Yong, Nanomaterials enhanced surface plasmon resonance for biological and chemical sensing applications, *Chem. Soc. Rev.* 43 (2014) 3426–3452.
- [3] M. Xu, T. Liang, M. Shi, H. Chen, Graphene-like two-dimensional materials, *Chem. Rev.* 113 (2013) 3766–3798.
- [4] Q.H. Wang, K. Kalantar-Zadeh, A. Kis, J.N. Coleman, M.S. Strano, Electronics and optoelectronics of two-dimensional transition metal dichalcogenides, *Nat. Nanotechnol.* 7 (2012) 699–712.
- [5] M. Chhowalla, H.S. Shin, G. Eda, L.-J. Li, K.P. Loh, H. Zhang, The chemistry of two-dimensional layered transition metal dichalcogenide nanosheets, *Nat. Chem.* 5 (2013) 263–275.
- [6] G. Eda, S.A. Maier, Two-dimensional crystals: managing light for optoelectronics, *Acs Nano* 7 (2013) 5660–5665.
- [7] K.S. Novoselov, A.H.C. Neto, Two-dimensional crystals-based heterostructures: materials with tailored properties, *Phys. Scripta* T146 (2012) 014006.
- [8] L. Yu, Y.-H. Lee, X. Ling, E.J.G. Santos, Y.C. Shin, Y. Lin, M. Dubey, E. Kaxiras, J. Kong, H. Wang, T. Palacios, Graphene/MoS<sub>2</sub> hybrid technology for large-scale two-dimensional electronics, *Nano Lett.* 14 (2014) 3055–3063.
- [9] K.V. Sreekanth, S. Zeng, J.Z. Shang, K.T. Yong, T. Yu, Excitation of surface electromagnetic waves in a graphene-based Bragg grating, *Scientific Rep.* 2 (2012) 737.
- [10] J. Xia, X. Huang, L.-Z. Liu, M. Wang, L. Wang, B. Huang, D.-D. Zhu, J.-J. Li, C.-Z. Gu, X.-M. Meng, CVD synthesis of large-area, highly crystalline MoSe<sub>2</sub> atomic layers on diverse substrates and application to photodetectors, *Nanoscale* 6 (2014) 8949–8955.
- [11] K.S. Novoselov, A.K. Geim, S.V. Morozov, D. Jiang, Y. Zhang, S.V. Dubonos, I.V. Grigorieva, A.A. Firsov, Electric field effect in atomically thin carbon films, *Science* 306 (2004) 666–669.
- [12] D.C. Elias, R.V. Gorbachev, A.S. Mayorov, S.V. Morozov, A.A. Zhukov, P. Blake, L.A. Ponomarenko, I.V. Grigorieva, K.S. Novoselov, F. Guinea, A.K. Geim, Dirac cones reshaped by interaction effects in suspended graphene, *Nat. Phys.* 7 (2011) 701–704.
- [13] A. Hoggard, L.-Y. Wang, L. Ma, Y. Fang, G. You, J. Olson, Z. Liu, W.-S. Chang, P.M. Ajayan, S. Link, Using the plasmon linewidth to calculate the time and efficiency of electron transfer between gold nanorods and graphene, *Acs Nano* 7 (2013) 11209–11217.
- [14] J. Kim, H. Son, D.J. Cho, B. Geng, W. Regan, S. Shi, K. Kim, A. Zettl, Y.-R. Shen, F. Wang, Electrical control of optical plasmon resonance with graphene, *Nano Lett.* 12 (2012) 5598–5602.
- [15] J. Niu, Y.J. Shin, Y. Lee, J.-H. Ahn, H. Yang, Graphene induced tunability of the surface plasmon resonance, *Appl. Phys. Lett.* 100 (2012) 061116.
- [16] S. Lee, M.H. Lee, H.-j. Shin, D. Choi, Control of density and LSPR of Au nanoparticles on graphene, *Nanotechnology* 24 (2013) 275702.
- [17] N. Reckinger, A. Vlad, S. Melinte, J.-F. Colomer, M. Sarrazin, Graphene-coated holey metal films: tunable molecular sensing by surface plasmon resonance, *Appl. Phys. Lett.* 102 (2013) 211108.
- [18] A.M. Zaniowski, M. Schiriger, J.G. Lee, M.F. Crommie, A. Zettl, Electronic and optical properties of metal-nanoparticle filled graphene sandwiches, *Appl. Phys. Lett.* 102 (2013) 023108.
- [19] S. Zeng, K.-T. Yong, I. Roy, X.-Q. Dinh, X. Yu, F. Luan, A review on functionalized gold nanoparticles for biosensing applications, *Plasmonics* 6 (2011) 491–506.
- [20] S. Zeng, X. Yu, W.-C. Law, Y. Zhang, R. Hu, X.-Q. Dinh, H.-P. Ho, K.-T. Yong, Size dependence of Au NP-enhanced surface plasmon resonance based on differential phase measurement, *Sens. Actuators B-Chem.* 176 (2013) 1128–1133.
- [21] E. Wijaya, C. Lenaerts, S. Maricot, J. Hastañin, S. Habraken, J.-P. Vilcot, R. Boukherroub, S. Szunerits, Surface plasmon resonance-based biosensors: from the development of different SPR structures to novel surface functionalization strategies, *Curr. Opin. Solid State Mater. Sci.* 15 (2011) 208–224.
- [22] L. Wu, H.S. Chu, W.S. Koh, E.P. Li, Highly sensitive graphene biosensors based on surface plasmon resonance, *Opt. Exp.* 18 (2010) 14395–14400.
- [23] B. Song, D. Li, W.P. Qi, M. Elstner, C.H. Fan, H.P. Fang, Graphene on Au(111): a highly conductive material with excellent adsorption properties for high-resolution bio/nanodetection and identification, *Chemphyschem* 11 (2010) 585–589.
- [24] G.B. McGaughey, M. Gagne, A.K. Rappe, Pi-stacking interactions – alive and well in proteins, *J. Biol. Chem.* 273 (1998) 15458–15463.
- [25] S.H. Choi, Y.L. Kim, K.M. Byun, Graphene-on-silver substrates for sensitive surface plasmon resonance imaging biosensors, *Opt. Exp.* 19 (2011) 458–466.
- [26] R. Verma, B.D. Gupta, R. Jha, Sensitivity enhancement of a surface plasmon resonance based biomolecules sensor using graphene and silicon layers, *Sens. Actuators B-Chem.* 160 (2011) 623–631.
- [27] P.K. Maharana, R. Jha, Chalcogenide prism and graphene multilayer based surface plasmon resonance affinity biosensor for high performance, *Sens. Actuators B-Chem.* 169 (2012) 161–166.
- [28] H. Zhang, Y. Sun, S. Gao, J. Zhang, H. Zhang, D. Song, Novel graphene oxide-based surface plasmon resonance biosensor for immunoassay, *Small* 9 (2013) 2537–2540.
- [29] R.R. Nair, P. Blake, A.N. Grigorenko, K.S. Novoselov, T.J. Booth, T. Stauber, N.M.R. Peres, A.K. Geim, Fine structure constant defines visual transparency of graphene, *Science* 320 (2008) 1308.
- [30] O. Salihoglu, S. Balci, C. Kocabas, Plasmon-polaritons on graphene-metal surface and their use in biosensors, *Appl. Phys. Lett.* 100 (2012) 213110.
- [31] K. Roy, M. Padmanabhan, S. Goswami, T.P. Sai, G. Ramalingam, S. Raghavan, A. Ghosh, Graphene–MoS<sub>2</sub> hybrid structures for multifunctional photoresponsive memory devices, *Nat. Nanotechnol.* 8 (2013) 826–830.
- [32] P.T.K. Loan, W. Zhang, C.-T. Lin, K.-H. Wei, L.-J. Li, C.-H. Chen, Graphene/MoS<sub>2</sub> heterostructures for ultrasensitive detection of DNA hybridisation, *Adv. Mater.* 26 (2014) 4838–4844.
- [33] S. Bertolazzi, D. Krasnozhon, A. Kis, Nonvolatile memory cells based on MoS<sub>2</sub>/graphene heterostructures, *Acs Nano* 7 (2013) 3246–3252.
- [34] O. Lopez-Sanchez, D. Lembe, M. Kayci, A. Radenovic, A. Kis, Ultrasensitive photodetectors based on monolayer MoS<sub>2</sub>, *Nat. Nanotechnol.* 8 (2013) 497–501.
- [35] B. Radisavljevic, A. Radenovic, J. Brivio, V. Giacometti, A. Kis, Single-layer MoS<sub>2</sub> transistors, *Nat. Nanotechnol.* 6 (2011) 147–150.
- [36] K.F. Mak, C. Lee, J. Hone, J. Shan, T.F. Heinz, Atomically thin MoS<sub>2</sub>: a new direct-gap semiconductor, *Phys. Rev. Lett.* 105 (2010) 136805.
- [37] D.-S. Tsai, K.-K. Liu, D.-H. Lien, M.-L. Tsai, C.-F. Kang, C.-A. Lin, L.-J. Li, J.-H. He, Few-layer MoS<sub>2</sub> with high broadband photogain and fast optical switching for use in harsh environments, *Acs Nano* 7 (2013) 3905–3911.
- [38] W. Zhang, C.-P. Chuu, J.-K. Huang, C.-H. Chen, M.-L. Tsai, Y.-H. Chang, C.-T. Liang, Y.-Z. Chen, Y.-L. Chueh, J.-H. He, M.-Y. Chou, L.-J. Li, Ultrahigh-gain photodetectors based on atomically thin graphene–MoS<sub>2</sub> heterostructures, *Scientific Rep.* 4 (2014) 3826.
- [39] G. Giovannetti, P.A. Khomyakov, G. Brocks, V.M. Karpan, J. van den Brink, P.J. Kelly, Doping graphene with metal contacts, *Phys. Rev. Lett.* 101 (2008) 026803.
- [40] B. Sachs, L. Britnell, T.O. Wehling, A. Eckmann, R. Jalil, B.D. Belle, A.I. Lichtenstein, M.I. Katsnelson, K.S. Novoselov, Doping mechanisms in graphene–MoS<sub>2</sub> hybrids, *Appl. Phys. Lett.* 103 (2013) 251607.
- [41] L. Britnell, R.M. Ribeiro, A. Eckmann, R. Jalil, B.D. Belle, A. Mishchenko, Y.J. Kim, R.V. Gorbachev, T. Georgiou, S.V. Morozov, A.N. Grigorenko, A.K. Geim, C. Casiraghi, A.H.C. Neto, K.S. Novoselov, Strong light-matter interactions in heterostructures of atomically thin films, *Science* 340 (2013) 1311–1314.
- [42] X.S. Li, Y.W. Zhu, W.W. Cai, M. Borysiak, B.Y. Han, D. Chen, R.D. Piner, L. Colombo, R.S. Ruoff, Transfer of large-area graphene films for high-performance transparent conductive electrodes, *Nano Lett.* 9 (2009) 4359–4363.
- [43] Y.Y. Hui, X. Liu, W. Jie, N.Y. Chan, J. Hao, Y.-T. Hsu, L.-J. Li, W. Guo, S.P. Lau, Exceptional tunability of band energy in a compressively strained trilayer MoS<sub>2</sub> sheet, *Acs Nano* 7 (2013) 7126–7131.
- [44] M.N. Polyanskiy, Refractive index database, <http://refractiveindex.info>
- [45] E.D. Palik, *Handbook of Optical Constants of Solids*, Academic, New York, 1985.
- [46] B.D. Gupta, A.K. Sharma, Sensitivity evaluation of a multi-layered surface plasmon resonance-based fiber optic sensor: a theoretical study, *Sens. Actuators B-Chem.* 107 (2005) 40–46.
- [47] H. Raether, *Surface Plasmons on Smooth and Rough Surfaces and on Gratings*, Springer-Verlag, Berlin, 1988.
- [48] A. Castellanos-Gomez, N. Agrait, G. Rubio-Bollinger, Optical identification of atomically thin dichalcogenide crystals, *Appl. Phys. Lett.* 96 (2010) 213116.
- [49] M. Bruna, S. Borini, Optical constants of graphene layers in the visible range, *Appl. Phys. Lett.* 94 (2009) 031901.
- [50] M. Daimon, A. Masumura, Measurement of the refractive index of distilled water from the near-infrared region to the ultraviolet region, *Appl. Optics* 46 (2007) 3811–3820.
- [51] K.V. Sreekanth, K.H. Krishna, A. De Luca, G. Strangi, Large spontaneous emission rate enhancement in grating coupled hyperbolic metamaterials, *Scientific Rep.* 4 (2014) 6340.
- [52] K.V. Sreekanth, S. Zeng, K.-T. Yong, T. Yu, Sensitivity enhanced biosensor using graphene-based one-dimensional photonic crystal, *Sens. Actuators B-Chem.* 182 (2013) 424–428.
- [53] V.G. Kravets, F. Schedin, R. Jalil, L. Britnell, R.V. Gorbachev, D. Ansell, B. Thackray, K.S. Novoselov, A.K. Geim, A.V. Kabashin, A.N. Grigorenko, Singular phase nanooptics in plasmonic metamaterials for label-free single-molecule detection, *Nat. Mater.* 12 (2013) 304–309.
- [54] A.V. Kabashin, S. Patskovsky, A.N. Grigorenko, Phase and amplitude sensitivities in surface plasmon resonance bio and chemical sensing, *Opt. Exp.* 17 (2009) 21191–21204.
- [55] I. Pockrand, Surface plasma oscillations at silver surfaces with thin transparent and absorbing coatings, *Surface Sci.* 72 (1978) 577–588.

## Biographies

**Shuwen Zeng** received her Ph.D. from School of Electrical and Electronic Engineering at Nanyang Technological University. She is currently working as a Postdoctoral Fellow at CNRS-International-NTU-THALES Research Alliances (CINTRA)/UMI 3288, Singapore. Her main research interests focus on nanomaterials preparation and their sensing applications.

**Siyi Hu** is currently an exchange research student at School of Electrical and Electronic Engineering, Nanyang Technological University. She is also a Ph.D. student of the School of Science at Changchun University of Science and Technology. Her main research interests focus on enhanced surface plasmon resonance sensing based on nanomaterials.

**Jing Xia** is currently a Ph.D. student at Technical Institute of Physics and Chemistry, Chinese Academy of Sciences, Beijing, PR China. His main research interests are synthesis, characterization, and application of two-dimensional (2D) nanomaterials.

**Tommy Anderson** received his B.Eng. degrees from School of Electrical and Electronic Engineering at Nanyang Technological University. He is currently Ph.D. student at School of Electrical and Electronic Engineering, Nanyang Technological University. His main research interests focus on synthesis of carbon-based nanomaterials for cancer therapy.

**Xuan-Quyen Dinh** received his Ph.D. in physics from Ecole Normale Supérieure (ENS) de Cachan, FRANCE in 2007. He is currently the Deputy-director of CNRS International-NTU-Thales Research Alliance (CINTRA), Singapore. His research interests include sensing applications based on surface plasmon resonance (SPR) and fiber devices.

**Xiang-Min Meng** received his bachelor degree in physics from Lanzhou University. Then, he has been a member of the Lab of Atomic Imaging of Solids, Chinese Academy of Sciences (CAS). From 1998 to 1999, as a STA fellow, he worked in National Institute for Materials Sciences, Japan. From 2001 and 2003, he worked in

City University of Hong Kong. Since 2005, he became a professor of Technical Institute of Physics and Chemistry, CAS. His current research interests are preparation, structural characterization and property study of semiconductor nanomaterials.

**Philippe Coquet** received his Ph.D. in Electrical and Electronic Engineering at the University of Rennes in 1993. He is currently the Director of CNRS International-NTU-Thales Research Alliance (CINTRA), Singapore and a professor at University of Lille 1, France. His research interests include nanotechnology for biosensing and microfluidic applications.

**Ken-Tye Yong** received his Ph.D. from Chemical and Biological Engineering in SUNY at Buffalo in 2006. Following completion of his graduate studies, he did his post-doc at the Institute for Lasers, Photonics and Biophotonics from 2006 to 2009. He is currently an Assistant Professor at the Nanyang Technological University in the School of Electrical and Electronic Engineering. His research interests are in the area of nanomaterials for theranostic applications.